Asymmetric electrowetting—moving droplets by a square wave†

Shih-Kang Fan,*[a] Hanping Yang,[b] Tsu-Te Wang[a] and Wensyang Hsu[b]

Received 19th March 2007, Accepted 29th June 2007
First published as an Advance Article on the web 20th July 2007
DOI: 10.1039/b704084a

Here droplet oscillation and continuous pumping are demonstrated by asymmetric electrowetting on an open surface with embedded electrodes powered by a square wave electrical signal without control circuits. The polarity effect of electrowetting on an SU-8 and Teflon coated electrode is investigated, and it is found that the θ–V (contact angle–applied voltage) curve is asymmetric along the $V = 0$ axis by sessile drop and coplanar electrode experiments. A systematic deviation of measured contact angles from the theoretical ones is observed when the electrode beneath the droplet is negatively biased. In the sessile drop experiment, up to a 10° increment of contact angle is measured on a negatively biased electrode. In addition, a coplanar electrode experiment is designed to examine the contact angles at the same applied potential but opposite polarities on two sides of one droplet at the same time. The design of the coplanar electrodes is then expanded to oscillate and transport droplets on square-wave-powered symmetric (square) and asymmetric (polygon) electrodes to demonstrate manipulation capability on an open surface. The frequency of oscillation and the speed of transportation are determined by the frequency of the applied square wave and the pitch of the electrodes. Droplets with different volumes are tested by square waves of varied frequencies and amplitudes. The 1.0 μl droplet is successfully transported on a device with a loop of 24 electrodes continuously at a speed up to 23.6 mm s^{-1} when a 9 Hz square wave is applied.

Introduction

Droplet manipulation has been widely studied in recent years.[1–3] For a diversity of liquids, a droplet can be used as a controllable electrical,[4] optical,[5–7] or thermal[8] component depending on its correlated physical properties. Certainly, a droplet can also be regarded as an independent liquid compartment, where chemical and biological reactions take place, and applied to lab-on-a-chip or μ-TAS.[9,10]

Electrowetting is one of the mechanisms to drive droplets, which is advantageous as the size of the droplet shrinks down for increased surface to volume ratio. Electrowetting-based devices can be divided into two categories depending on the driving scheme and device structure. The first one is a sandwiched device, in which droplets are driven between two parallel plates.[11–13] Driving electrodes are usually patterned on one of the plates, and a reference electrode is on the other plate. The second one is an open device, where droplets are manipulated on a single plate containing both control and reference electrodes.[14–16]

However, in most electrowetting-based devices, transporting droplets for a long distance increases the number of electrodes as well as the complexity of the control circuit. Here we show a new droplet manipulation principle to oscillate and continuously pump a droplet on an open surface with embedded electrodes powered by simply a square wave electric signal without control circuits based on asymmetric electrowetting.

[a]*Institute of Nanotechnology, National Chiao Tung University, Hsinchu, Taiwan E-mail: skfan@mail.nctu.edu.tw; Fax: +886-3-5729912; Tel: +886-3-5712121 ext. 55813*
[b]*Department of Mechanical Engineering, National Chiao Tung University, Hsinchu, Taiwan*

† Electronic supplementary information (ESI) available: Fig. S1 and videos of droplet movement. See DOI: 10.1039/b704084a

Principle and fundamental studies

Sessile drop experiment

Electrowetting is an electrical means to alter the interfacial tension between electrodes and liquids.[17,18] When dealing with electrowetting on an insulator coated solid electrode, the relationship between the contact angle and the applied voltage is usually studied by a sessile drop experiment (see Fig. S1 in the ESI†) and described by Young–Lippmann equation:[19,20]

$$\cos\theta - \cos\theta_0 = \frac{1}{2}\frac{c}{\gamma_{LG}}V^2 \quad (1)$$

where θ_0 is the contact angle without applied voltage, θ is the contact angle corresponding to the applied potential V, c is the specific capacitance of the insulator layer, and γ_{LG} is the surface tension at the liquid–gas interface. In theory, the curve of contact angle (θ) *versus* the applied voltage (V) should be a symmetric parabola along the $V = 0$ axis before contact angle saturation.[19,21] In earlier studies, since an alternating current (a.c.) signal was usually applied,[20,22] the polarity effect of the applied direct current (d.c.) signal was rarely considered. However, with an 1 μm-thick SU-8 and 66 nm-thick Teflon coated indium tin oxide (ITO) bottom electrode and a Teflon coated platinum (Pt) probe, referred to in Fig. S1 in the ESI†, the experimental results of a 2.5 μl de-ionized (DI) water droplet show a systematic deviation from the symmetrical model at one side of the parabola (Fig. 1(a)). For sample

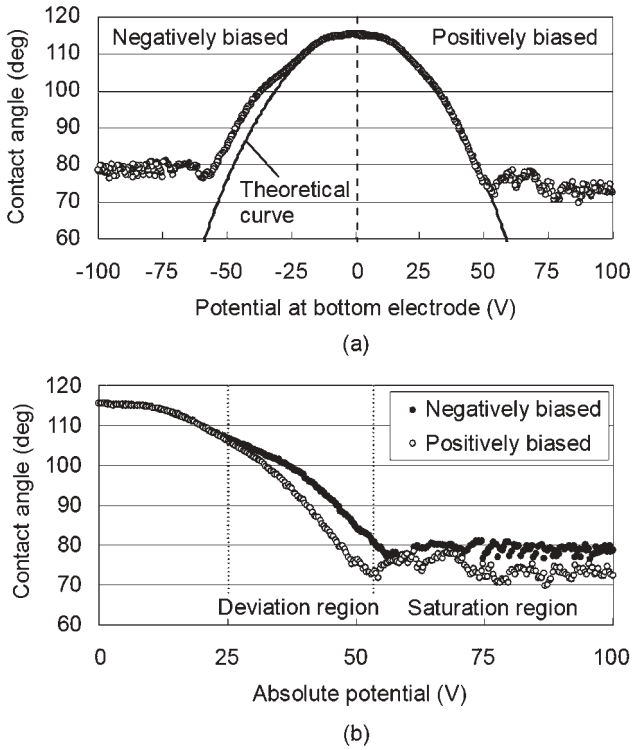

Fig. 1 Results of sessile drop experiment showing asymmetric electrowetting. (a) Measured contact angle from −100 V to 100 V. (b) Flipped curve showing the contact angle difference caused by polarity.

preparation, 1 μm-thick SU-8 (Gersteltec GM-1040) is spun on an ITO substrate and then baked at 90 °C for 5 min. The sample is subsequently exposed to a 500% over dosage (500 mJ cm^{-2}) and baked again at 90 °C for 5 min. After development the SU-8 insulator is obtained with patterned electric contact windows. Finally, 66 nm-thick Teflon is coated by spinning FC-77 dissolved 1 wt% AF 1600 at 2000 rpm for 25 s and dried in ambiance. It is found that when a sufficient negative potential is applied on the bottom electrode, deviation of measured contact angles from the theoretical ones (solid line in Fig. 1(a)) results in a gentler sloped θ–V curve at the left side of the parabola. The polarity sensitive electrowetting, causing an asymmetric curve along the $V = 0$ axis, is called "asymmetric electrowetting." Fig. 1(b) highlights the contact angle difference caused by polarity. In the deviation region, the contact angle difference is up to 10° before entering saturation region. In the saturation region, the jittering of contact angle occurs due to droplet motion around the Teflon-coated probe at high voltage. A similar asymmetric electrowetting curve is observed more than five times in our experiments.

The material used for insulator has direct effect in asymmetric electrowetting. Parylene has been widely used both in fundamental studies[23,24] and device applications[13,25] of electrowetting. It was reported that while using Parylene as the insulator, the change in contact angle was independent of the polarity.[24] It is verified here by simply replacing the SU-8 layer with Parylene and no asymmetric electrowetting is observed. Researchers noticed the asymmetry of electrowetting when removing Parylene and using only Teflon as insulator.[26] Three grades of Teflon ware compared by Quinn *et al.*[27] and the composition of the Teflon influenced the asymmetry of electrowetting. The deviation of measured contact angle was observed at positive potentials when PDD (4,5-difluoro-2,2-bis(trifluoromethyl)-1,3-dioxole) existed in Teflon. It was suggested that the OH^- ions have higher affinity towards the oxygen atoms in PDD and cause adsorbed or trapped charge on or in Teflon, which reduces the electrowetting force when the bottom electrode is positively biased. At negative potentials, the OH^- ions are electrostatically repelled, and no deviation is noticed. However, SU-8 is an epoxy-based negative photoresist, which consists of epoxies and photo-initiators (triarylsulfonium salts).[28] After exposure, SU-8 is polymerized by cationic photopolymerization processes, which releases hexafluoroantimonate complexes (SbF_6^-) from photoinitiators for further polymerization processes. In our experiment, the SU-8 is exposed by a 500% over dosage, meaning most of the photoinitiator is reacted, and then generates large amount of SbF_6^-. The SbF_6^- is suggested to be the cause of the negative surface charge of SU-8.[29] We speculate that cations would be adsorbed or trapped by SbF_6^- on Teflon or in SU-8, reducing electrowetting, especially when the bottom electrode is negatively biased. However, more studies are required to understand the physics of the phenomenon. Here we focus on its application of droplet manipulations.

Coplanar electrode experiment

To further study the asymmetric electrowetting phenomenon without the effect of the top probe in the sessile drop experiment and be able to observe the contact angle difference caused by the electric polarity on a single droplet at the same time, an experiment on patterned coplanar electrodes is designed, as shown in Fig. 2. Three coplanar electrodes, *i.e.*, H-shaped (90°-rotated), right-strip, and left-strip electrodes (Fig. 2(a)), are designed and patterned on an ITO substrate. The ITO electrodes are covered with 1 μm-thick SU-8 and 66 nm-thick Teflon, referred to in Fig. 2(b), with the same procedure described above. A 4 μl droplet is first placed on the electrodes and positioned at the center (dashed circle in Fig. 2(a)). After positioning, the left-strip electrode is kept grounded, while a stepped voltage from 0 V to 120 V is applied to the right-strip electrode. The contact angles on the left- and right-strip electrodes, denoted as θ_L and θ_R respectively in Fig. 2(b), are measured and analyzed from the recorded front views and plotted in Fig. 2(c). The deviation of θ_L and θ_R becomes obvious at voltages over 30 V, and increases gradually to the maximum of 8.98° at 70 V where θ_L and θ_R are 100.94° and 91.96°, respectively. It is worth to notice that θ_L is 96.51° (>90°), and θ_R is 88.1° (<90°) at 80 V, that means the left side is hydrophobic, and the right side is hydrophilic.

Electrical analysis

Unlike the sessile drop experiment, when applying voltage on a pair of coplanar electrodes, the voltage across the capacitor above each electrode no longer equals the applied voltage. A simplified equivalent circuit, containing two capacitors C_L and C_R in series to describe this experiment is shown in Fig. 2(b).

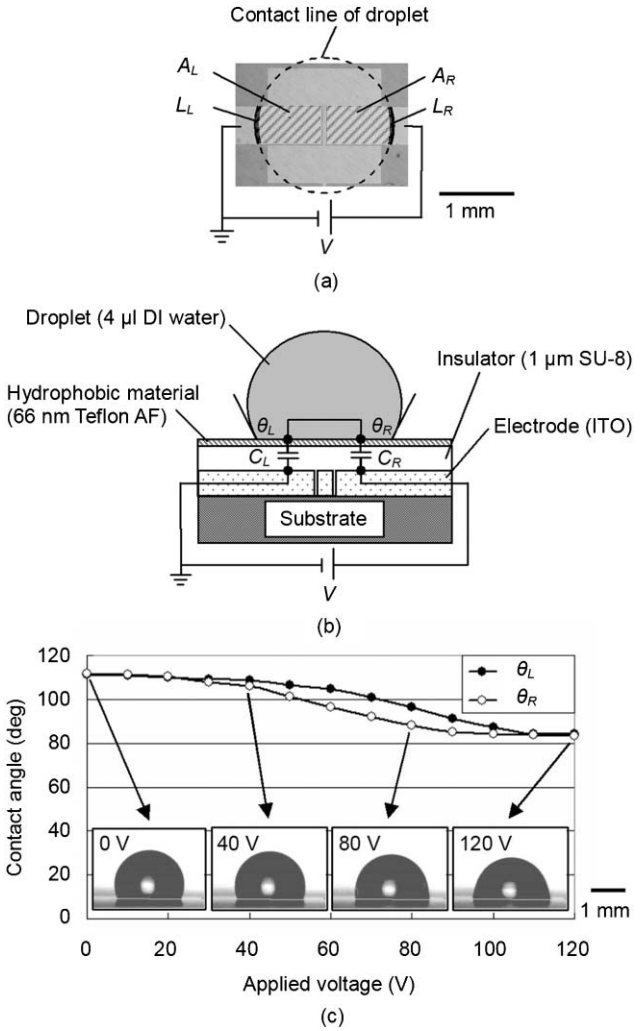

Fig. 2 Coplanar electrode experiment for observation of two contact angles of a droplet applied with opposite polarities. (a) Top view, showing the H-shaped, left-strip, and right-strip coplanar electrodes, and droplet position (dashed line). (b) Cross-sectional view, revealing the device configuration and simplified equivalent circuit. (c) Measured θ_L and θ_R of applied V from 0 to 120 V. The insets are front views of the measured droplet of 0, 40, 80 and 120 V applied voltages.

By considering the overlapping areas A_L and A_R as equal, the external applied voltage, V, would be distributed evenly on C_L and C_R ($V_L = V_R = V/2$). Although V_L and V_R are equal, their polarities are opposite: the left-strip electrode is always negatively biased, while the right-strip one is positively biased. Therefore, θ_L is greater than or equal to θ_R. Assuming the overlapping meniscus lengths L_L and L_R are equal to L, when there is a contact angle difference, a surface tension force, F, would exert on the droplet and can be described as:

$$F = \gamma_{LG} \times L(\cos\theta_R - \cos\theta_L). \quad (2)$$

The design of the strip electrodes in the experiment is to reduce L and F. Since contact angle hysteresis still exists, a small F would still keep the droplet stationary during the experiment for contact angle analyses.[30]

Experiments

Droplet oscillation

By increasing the width of the strip electrodes, the force F caused by asymmetric electrowetting would increase and be able to overcome the hysteresis phenomenon and drive the droplet. A pair of square electrodes are designed and fabricated to verify the concept in droplet oscillating experiment, as shown in Fig. 3. A 1.5 μl droplet is carefully dispensed between the electrodes (dashed circle in Fig. 3(a)). As in the previous coplanar electrode experiment, the left electrode is electrically grounded and 70 V is applied to the right electrode (Fig. 3(a)). 70 V is chosen for its high contact angle difference based on the results in Fig. 2. As we expected, the droplet moves to the right electrode, which is positively biased. Then the potential is reversed, as shown in Fig. 3(b). The droplet is found to move back to the left. When a square wave is applied on the pair of the electrodes, the polarity on each electrode would be changed regularly and continuously. As a result, the droplet would be driven back and forth on the electrodes. Fig. 3(c) shows a frame of a 15 Hz-oscillated droplet at the recorded frame rate of 30 fps. Interestingly, the frequency of the droplet oscillation is decided by the frequency of the square

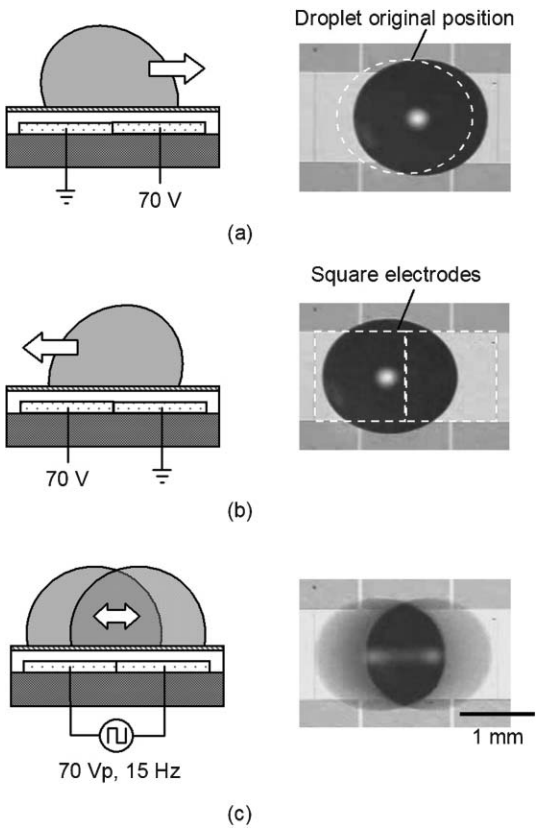

Fig. 3 Droplet (1.5 μl DI water) oscillating experiment on a pair of symmetric (square) electrodes. (a) Droplet moves to the right by applying 70 V on the right electrode and electric ground on the left one. Dashed circle is the original position of droplet (b) Droplet is moved to the left by switching the wire connections. Dashed squares are the symmetric electrodes underneath the droplet. (c) Droplet oscillation performed by a square wave.

wave. A high speed camera is required for studying droplet oscillation at higher frequencies in the future.

Droplet continuous pumping

Not only droplet oscillation but also continuous droplet pumping is possible by asymmetric electrowetting. The asymmetric (polygon) electrodes are designed to be composed of a small square and a large square as shown in Fig. 4(a). Electrodes in a series are divided into two groups and connected to the two terminals of a square wave. From the previous studies, when a square wave was applied on symmetric (square) electrodes, the droplet above them would oscillate. However, when applying a square wave on asymmetric electrodes, the asymmetry would continuously pump the droplet in a certain direction, as shown in Fig. 4(a). A liquid droplet is first placed on electrodes 1 and 2 (at $t = 0$), and a square wave with period T is applied subsequently. In the first half period ($t = 0$–$T/2$), since electrode 2 carries a positive potential compared with electrode 1, the droplet tends to move toward it. If the applied voltage is sufficient, the droplet will be pumped thoroughly onto electrode 2 and touch both electrode 2 and 3. Similarly, in the rest half period of the first one ($t = T/2$–T), the droplet will be pumped one electrode further to the left (electrode 3). Therefore, the droplet is pumped two electrodes every square wave period. The pumping speed is determined by the size of electrodes and the frequency of square wave.

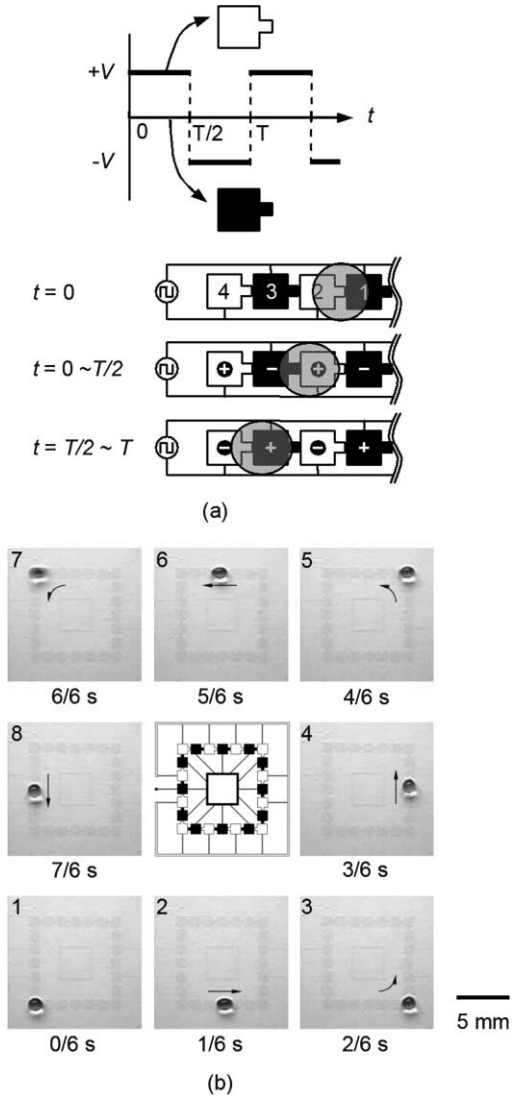

Fig. 4 Droplet continuous pumping on a loop of asymmetric (polygon) electrodes. (a) Electrode design and driving scheme for droplet continuous pumping by a square wave. (b) Continuous pumping test. A 1.0 μl DI water droplet is successfully pumped on a loop of 24 asymmetric electrodes continuously at the speed of 23.6 mm s^{-1} when a 90 Vp and 9 Hz square wave is applied.

A loop of 24 coplanar asymmetric electrodes is designed for continuous pumping of droplets on an open surface. Only two contact pads are required in this design for droplet manipulation on 24 electrodes. The big square of the asymmetric electrode is 1 mm wide, and the small square is 0.3 mm wide. Each electrode is spaced 10 μm apart. Fig. 4(b) shows the video frames of a continuously pumped 1.5 μl droplet along the electrode loop by a 90 Vp and 9 Hz square wave. As expected, it takes 4/3 s for a droplet to accomplish one loop at the speed of 23.6 mm s^{-1} when 9 Hz square wave drives droplets at a rate of 18 electrodes per second.

Discussion

Besides successfully continuous pumping, two other droplet motions are observed during the test, including oscillation and irregular motion. Fig. 5(a) shows the three kinds of motion of an 1.5 μl droplet while applying 1 Hz square waves with different voltages. Since the sequential pictures are shown at an interval of 0.25 s, the polarity of the electrodes is switched every other picture. At 40 Vp, the droplet slightly oscillates between two electrodes, as shown in Fig. 5(a), because the small contact angle difference provides insufficient surface tension force to pump the whole droplet from one electrode to another. The contact angle difference can be roughly estimated from Fig. 2. At 90 Vp, asymmetric electrowetting causes a sufficient contact angle difference, and pumps the droplet continuously. In the 2 s span of the pictures, the droplet is pumped 4 electrodes by the 1 Hz square wave. At 140 Vp, droplet expansion and contraction is observed mostly, but irregularly. It is speculated that the voltage is too high and leads to contact angle saturation, reducing the asymmetric electrowetting effect. Contractions of the droplet are caused by the changes of polarity. For the high voltage and the abrupt voltage change of square wave, sometimes the droplet jumped one step to its right or left at the moment of polarity change.

Three kinds of motion are further studied systematically for droplets of various volumes by square waves with different amplitudes and frequencies. As shown in Fig. 5(b), both 1 μl and 1.5 μl droplets are able to be pumped continuously. (At $\theta = 115°$ ($V = 0$), the droplet contact area to electrode area ratios are 1.06 and 1.39 for 1 μl and 1.5 μl droplets.) Smaller droplets are found to have a broader operation range for continuous pumping. However, droplets less than 1 μl are prone to stick on one electrode, because they are too small to cover two electrodes. On the other hand, droplets with excess volume

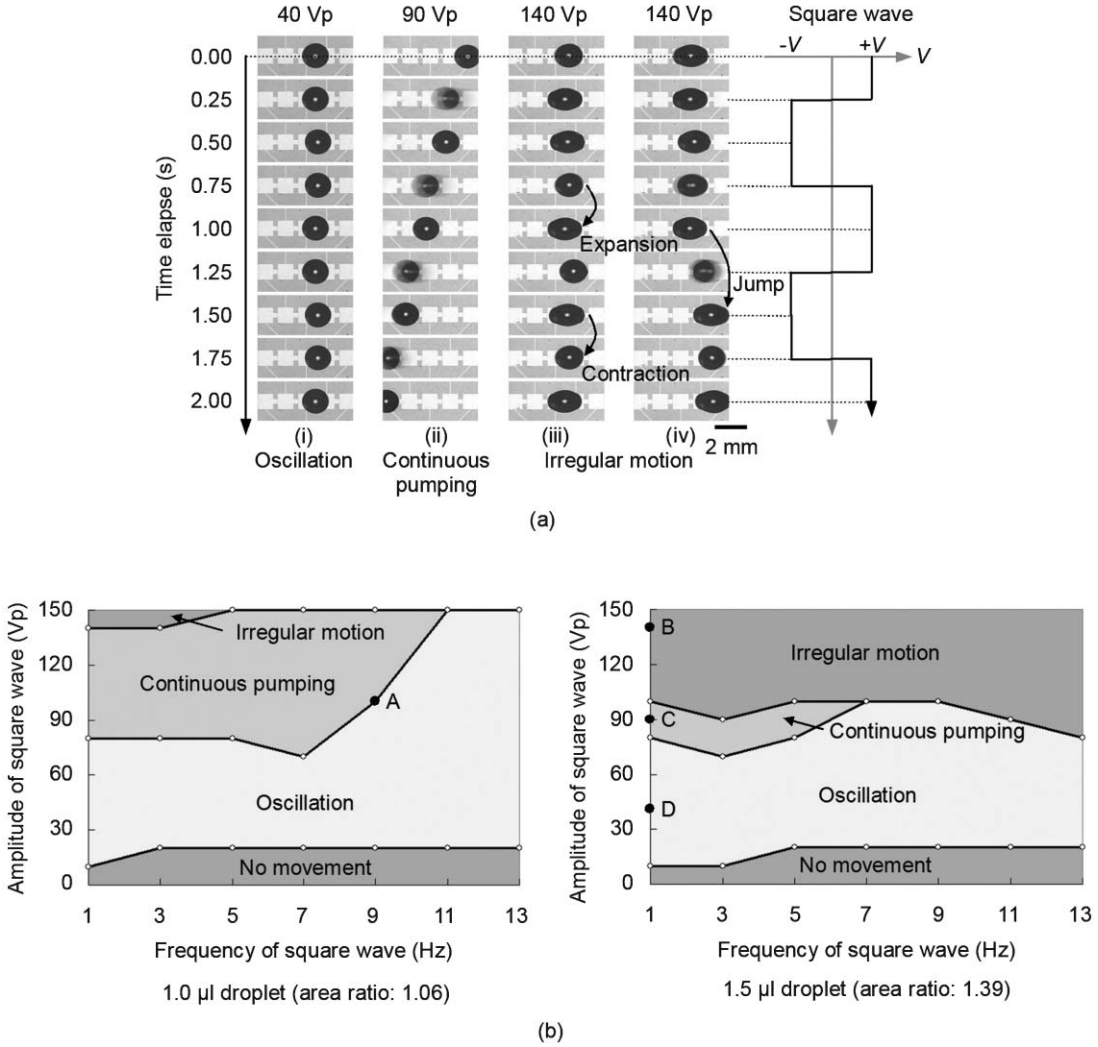

Fig. 5 Droplet actuation tests. (a) Three kinds of motion of an 1.5 μl droplet driven by 1 Hz square waves with amplitude of 40 Vp, 90 Vp, and 140 Vp respectively. (b) Droplet motions of 1.0 μl and 1.5 μl droplets by square wave with different frequency and amplitude. Square waves of frequencies from 1 Hz to 13 Hz with an interval of 2 Hz were tested. At a certain frequency, the amplitude was applied from 0 Vp to 150 Vp with an interval of 10 V. The dots on the broken line show the minimum voltage to enter the above motion region. For example, dot A is the result of Fig. 4(b). In addition, dots B, C, and D are the results shown in (a).

(*e.g.*, 2 μl) would cover more than two electrodes and oscillate between covered electrodes.

Conclusions

Asymmetric electrowetting is observed and studied by sessile drop and coplanar electrode experiments. It is found that the electrowetting phenomenon is polarity sensitive and asymmetric on an SU-8 and Teflon coated electrode. When applying a square wave electric signal on a pair of coplanar symmetric (square) electrodes, the regularly changed polarity oscillates the droplet above. Moreover, droplet continuous pumping on an open surface is achieved by a loop of asymmetric (polygon) electrodes powered by a square wave. The droplet motion on asymmetric electrodes depends on the volume of the droplet, frequency, and amplitude of the square wave. Therefore, droplets with appropriate volumes can be pumped or oscillated by a right frequency and amplitude combination. The demonstrated asymmetric-electrowetting-based droplet manipulation distinguishes itself from other methods by a simple actuation mechanism, driving scheme and device configuration.

References

1 M. Joanicot and A. Ajdari, *Science*, 2005, **309**, 887–888.
2 S. Daniel, M. K. Chaudhury and J. C. Chen, *Science*, 2001, **291**, 633–636.
3 H. Linke, B. J. Alemán, L. D. Melling, M. J. Taormina, M. J. Francis, C. C. Dow-Hygelund, V. Narayanan, R. P. Taylor and A. Stout, *Phys. Rev. Lett.*, 2006, **96**, 154502.
4 J. Simon, S. Saffer and C.-J. Kim, *J. Microelectromech. Syst.*, 1997, **6**, 208–216.
5 S. X. Qian, J. B. Snow, H. M. Tzeng and R. K. Chang, *Science*, 1986, **231**, 486–488.
6 R. A. Hayes and B. J. Feenstra, *Nature*, 2003, **425**, 383–385.
7 S. Kuiper and B. H. W. Hendriks, *Appl. Phys. Lett.*, 2004, **85**, 1128–1130.

8 V. K. Pamula and K. Chakrabarty, *Proc. 13th ACM Great Lakes Symposium on VLSI*, Washington D. C., USA, 2003, pp. 84–87.
9 V. Srinivasan, V. K. Pamula and R. B. Fair, *Lab Chip*, 2004, **4**, 310–315.
10 J. R. Millman, K. H. Bhatt, B. G. Prevo and O. D. Velev, *Nat. Mater.*, 2005, **4**, 98–102.
11 S. K. Cho, H. Moon and C.-J. Kim, *J. Microelectromech. Syst.*, 2003, **12**, 70–80.
12 M. G. Pollack, R. B. Fair and A. D. Shenderov, *Appl. Phys. Lett.*, 2000, **77**, 1725–1726.
13 M. G. Pollack, A. D. Shenderov and R. B. Fair, *Lab Chip*, 2002, **2**, 96–101.
14 U. -C. Yi and C. -J. Kim, *J. Micromech. Microeng.*, 2006, **16**, 2053–2059.
15 A. Torkkeli, J. Saarilahti, A. Haara, H. Harma, T. Soukka and P. Tolonen, *Proc. IEEE Int. Conf. on Micro Electro Mechanical Systems, MEMS 2001*, Interlaken, Switzerland, 2001, pp. 475–478.
16 T. T. Wang, P. W. Huang and S. K. Fan, *Proc. IEEE Int. Conf. on Micro Electro Mechanical Systems, MEMS 2006*, Istanbul, Turkey, 2006, pp. 174–177.
17 C. Quilliet and B. Berge, *Curr. Opin. Colloid Interface Sci.*, 2001, **6**, 34–39.
18 F. Mugele and J.-G. Baret, *J. Phys.:Condes. Matter*, 2005, **17**, R705–R774.
19 B. Berge, *C. R. Acad. Sci. Ser. II: Mec., Phys., Chim., Sci. Terre Univers*, 1993, **317**, 157–163.
20 M. Vallet, B. Berge and L. Vovelle, *Polymer*, 1996, **37**, 2456–2470.
21 M. Vallet, M. Vallade and B. Berge, *Eur. Phys. J.*, 1999, **11**, 583–591.
22 L. Minnema, H. A. Barneveld and P. D. Rinkel, *IEEE Trans. Electr. Insul.*, 1980, **EI-15**, 461–472.
23 W. J. J. Welters and L. G. J. Fokkink, *Langmuir*, 1998, **14**, 1535–1538.
24 H. J. J. Verheijen and M. W. Prins, *Langmuir*, 1999, **15**, 6616–6620.
25 Z. Wan, H. Zeng and A. Feinerman, *Appl. Phys. Lett.*, 2006, **89**, 201107.
26 E. Seyrat and R. A. Hayes, *J. Appl. Phys.*, 2001, **90**, 1383–1386.
27 A. Quinn, R. Sedev and J. Ralston, *J. Phys. Chem. B*, 2003, **107**, 1163–1169.
28 J. M. Shaw, J. D. Gelorme, N. C. LaBianca, W. E. Conley and S. J. Holmes, *IBM J. Res. Dev.*, 1997, **41**, 81–94.
29 T. Sikanen, S. Tuomikoski,, R. A. Ketola,, R. Kostiainen, S. Franssila and T. Kotiaho, *Lab Chip*, 2005, **5**, 888–896.
30 E. B. Dussan and R. T.-P. Chow, *J. Fluid Mech.*, 1983, **137**, 1–29.